Proceedings 10th NUMGE 2023
10th European Conference on Numerical Methods in Geotechnical Engineering
Zdravkovic L, Kontoe S, Taborda DMG, Tsiampousi A (eds)

https://doi.org/10.53243/NUMGE2023-139

Numerical limit analyses of the vertical capacity of plate anchors in clay

E. Varela[1], M. Miranda[1], J. Castro[1], A. Da Costa[1], J. Cañizal[1]

[1]*Group of Geotechnical Engineering, University of Cantabria*

ABSTRACT: The increasing demand of renewable energy sources and the efficiency of wind energy has promoted the development of offshore wind energy to exploit deep-sea winds, as well as avoid the visual impact that onshore wind farms create. Floating platforms are an efficient and economical option for deep waters and plate anchors are commonly used in their mooring systems. In this research, 2D and 3D finite element analyses of the vertical pull-out capacity of plate anchors in purely cohesive soils are performed at different embedment ratios. The study is simplified to a homogeneous weightless soil layer with constant undrained shear strength. The codes OptumG2 and OptumG3 were used with satisfactory results, because they allow to progressively refine the finite element mesh (adaptative mesh refinement) and perform elastoplastic analysis and upper and lower bound limit analysis. Axisymmetric and plane strain models for two dimensions (circular and strip anchors) and circular and square shapes in three dimensions were analysed. Results include visualization of the failure mechanisms and values of the pull-out capacity expressed as a dimensionless break-out factor. These values are compared with analytical solutions.

Keywords: plate anchors; numerical analysis; finite elements; upper and lower bound analysis; offshore wind energy.

1 INTRODUCTION

The increasing demand of renewable energy sources and the need for installation space has led to the search for new locations. Wind energy has undergone major development in recent decades and, with the intention of capturing offshore winds, the offshore wind energy industry has also developed enormously (Randolph and Gouvernec, 2011).

For offshore wind farm locations at large depths (over 50 meters), floating platforms with mooring systems are the best solution. Different types of anchors can be used and plate anchors, specifically SEPLA (Suction Embedded Plate Anchors) are a common option. Plate anchors can have different shapes, with square and circular being two simple and functional designs (Roy et al. 2020).

In this publication, three-dimensional finite element (FE) numerical analyses are performed to compare circular and square shaped anchors. In addition, two-dimensional analyses are performed, mesh sensitivity analyses are done, and the results are compared with those obtained by other authors to validate the numerical models.

2 STATE OF ART

The usual procedure for studying the behaviour of plate anchors is to obtain a break out factor that permits comparing results from anchors of different characteristics (shape, depth, roughness, etc.). This parameter is based on factors used for superficial footings and is obtained from the vertical pull-out load and the undrained shear resistance of the soil:

$$q_u = \frac{Q_u}{A} = c_u N_c \qquad (1)$$

where A is the anchor area, c_u is the undrained shear resistance and N_c is the break out factor, which is dependent on the unit weight of the soil. It can be separated in two addends:

$$N_c = N_{c0} + \frac{\gamma z}{c_u} \qquad (2)$$

where $N_{c0} = \left(\frac{q_u}{c_u}\right)_{\gamma=0}$ is the break out factor for a weightless soil, and, therefore, independent of it.

One of the objectives of this study is to obtain the N_{c0} break out factor for a series of cases, namely, different anchor types and varying normalized depths, *z/B*. This is why in this study a weightless soil is considered.

The value of the break out factor does not increase indefinitely, it reaches a maximum value, defined as N^*_c ($=N^*_{c0}$) and corresponds with the transition between a superficial failure mechanism with a deep one. The latter does not depend on depth and has a constant value.

2.1 General anchor behaviour

Rowe and Davis (1982) divided anchor behaviour in two categories: those that separate from the soil when subjected to pull-out (breakaway) and those that do not separate (no breakaway). For the first case, the interface between the anchor and the soil does not sustain traction and, therefore, the stresses on the bottom side of the anchor are null. When subject to vertical pull-out the anchor will immediately detach from the soil on its bottom side, with no suction occurring. This condition known as "vented condition", is considered in this publication, as other authors have done, such as Merifield (2003), Martin and Randolph (2001) and Yu et al. (2011), because it results in a conservative value. In this study, the effect of the roughness of the anchor is also analysed.

2.2 Previous studies

Over the last five decades a good number of studies on the behaviour of plate anchors in clays have been published.

Martin and Randolph (2001) studied analytical plastic solutions for circular buried plate foundations in two dimensions (assuming axial symmetry) in a homogeneous soil of infinite extension. These foundations are equivalent to plate anchors that have been "wished in place" (which implies that the installation process, or keying process, is not considered) and have applied the vented condition, same as this study. Therefore, their solution corresponds to the deep failure mechanism. They apply upper and lower bound limit equilibrium theorems and obtain the maximum value of the break out factor, N^*_{c0}, for two opposite cases of roughness: rough and smooth interfaces.

Merifield (2003) performed analytical analyses in three dimensions for circular and square plate anchors in undrained clays, comparing its results with other authors, using a limit analysis method based on classic plasticity theorems developed by Drucker et al. (1952). The same conditions (wished in place and vented condition) have been considered. The study was done for a large range of depths.

Martin (2009) studied the trapdoor problem in clays in plane strain conditions that is elevated vertically, which is equivalent to plate anchors as well. The solution (Equation 3) coincides with the superficial failure mechanism and is a more precise adjustment than the classical solution proposed by Davis (1968) (Equation 4):

$$N_c = 1.956\frac{z}{B} \quad (3)$$

$$N_c = 2\frac{z}{B} \quad (4)$$

Martin (2009) also provides upper and lower bound plane strain numerical analysis results in clay. These values will be compared with the results of this study.

3 NUMERICAL MODEL

In this section, the numerical model, the parameters and chosen numerical analysis finite element program are described. Two anchor shapes were analysed, namely circular and square. Two and three-dimensional analyses were done, therefore, for the 2D models, hypothesis of axial symmetry and plane strain are assumed. In 2D a square shaped anchor cannot be analysed, only strip anchors. A comparison between 2D and 3D results can be done with the circular anchor analyses results.

Figure 1 shows the variables present in the model, where B is the side length of the square anchor. For the circular anchors, a diameter D is chosen so that the area of both anchor shapes is the same:

$$D = \frac{2B}{\sqrt{\pi}} \quad (5)$$

The vertical pull-out is applied as a uniform distributed displacement on the surface of the anchor. The thickness of the anchor is considered negligible, since it is modelled as a rigid plaque with two interfaces that control the contact between the anchor and the soil. The analysis is done in undrained conditions; therefore, the undrained shear strength c_u is used. The results of the analyses will be a series of values of the break-out factor.

For the model, the following two hypotheses are made: the anchor is "wished in-place" and the "vented condition". Lastly, the unit weight of the soil is considered zero. Therefore, the expression to obtain the dimensionless break out factor is:

$$N_{c0} = \frac{Q}{A\, c_u} \quad (6)$$

where A is the area of the anchors, the same for both shapes, c_u is the undrained shear strength, and Q is the vertical pull-out force, which is the result of the numerical analyses.

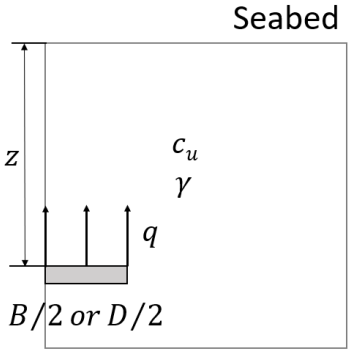

Figure 1. Model variables

3.1 Numerical analysis software

For the numerical analyses the numerical code OPTUM, in its two versions for two-dimensional and three-dimensional calculations, was used (Krabbenhoft et al.

2015). These codes integrate interesting tools such as adaptative mesh refinement, which reduces the size of the elements in the areas of the model where displacements occur; or the possibility of performing upper and lower bound analysis as well as conventional elasto-plastic analysis.

The adaptative mesh refinement permits creating initial models with less elements and the software performs iterations of the calculations on each step, it identifies the areas of the model where displacements or stress increments occur, and refines the mesh. These maximizes the precision of the result while reducing the computational cost (Figure 2). On the other hand, comparing the upper and lower bound limit analysis with the elasto-plastic analysis, the former reduces the computational time and provides two solutions that delimit the exact solution, being the difference between the both the precision of the calculation.

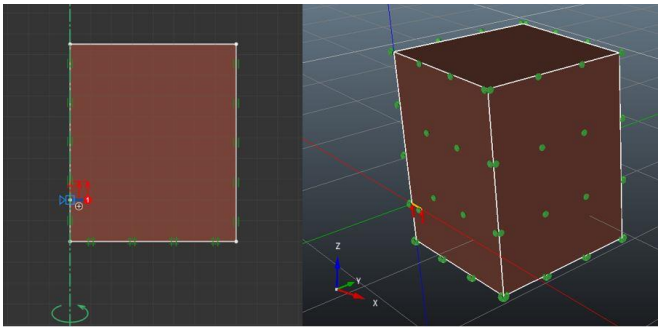

Figure 2. 2D OPTUM view (left). 3D OPTUM view (right).

3.2 Model characteristics

Even though the results of these analyses are presented in the form of a dimensionless factor N_{c0}, the creation of the model has to be dimensional and certain parameters have to be introduced in the numerical code.

The size of the model has to be large enough to guarantee that the boundary conditions do not affect the results. A sensitivity analysis is done to study the size of the model for different target embedment depths, resulting in a model width of 3.3 times the anchor size B for z/B=1 and a width of 20 times B for z/B=20.

The soil is a perfect elasto-plastic Tresca type material. The following parameters are used for soil: $\gamma = 0$, $c_u = 50\ kPa$, $\nu_u = 0.5$ and $E_u = 1x10^6\ MPa$. The unit weight is considered zero as explained previously. Poisson's coefficient is usually taken as a value close to 0.5 to avoid numerical convergences in conventional elasto-plastic calculations. However, with upper and lower bound limit analyses this issue is not a problem. The elevated value for the undrained Young's modulus was chosen to reproduce a rigid-plastic behaviour.

In order to model the vented condition on the bottom side of the anchor, the value of the traction resistance on the interface is set to zero. The anchor is modelled as an infinitely thin rigid plate with two interfaces. The adhesion value of this interfaces can be varied between zero and the undrained shear strength c_u. In order to have a completely smooth anchor surface, this adhesion should be null.

The reference anchor is a square shaped anchor with a side length of B=1.5m. Therefore, the circular anchor will have a diameter D of D=1.69m. Other publications take for simplicity D=B. Moreover, the embedment ratio for both anchors are identical and referred to the factor $z/\sqrt{A} = z/B$.

In both cases, symmetry conditions are exploited. In 2D models, half of the anchor is modelled, one radius for axisymmetric conditions (circular anchor) and half the width for plane strain conditions. In 3D models, one fourth of the anchor is modelled in both cases.

3.3 Calculation precision

As mentioned previously, OPTUM in both versions for two and three-dimensional analysis, has the possibility of performing upper (UB) and lower bound (LB) limit analyses. The precision of the model is indicated by the difference between those values.

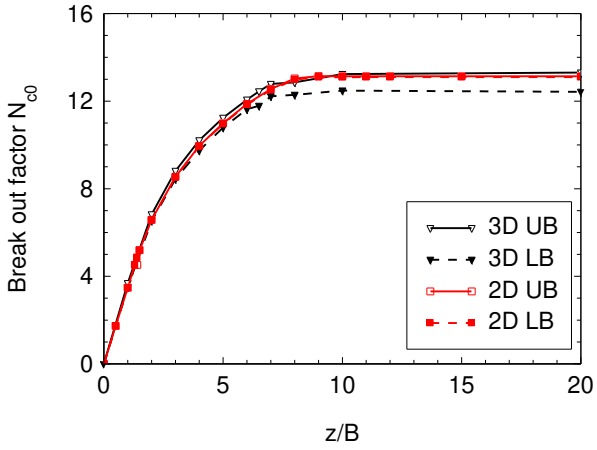

Figure 3. Break out factor for circular shaped anchors, in two and three dimensions.

Figure 3 shows the results of the numerical analyses done for circular anchors in both two and three dimensions. It is observed how the results almost coincide (differences lower than 1%) if the study is done in axial symmetry in two dimensions, which practically gives the exact solution with ample precision. The three-dimensional analyses require a reasonable reduction in number of elements and lowering the order of these. For reduced depths, the results in two and three dimensions are practically equal. However, for larger depths, the differences increase. The differences between the maximum values for upper and lower bound analyses are as high as 6% in three dimensions and lower than 1% in two dimensions. This can be associated with the size of the model, and, therefore, the increase in the average size of the finite elements, if the number of elements is similar.

4 RESULTS

4.1 Two-dimensional analyses

The values of the break out factor obtained are represented in Figure 4 and Figure 5. The results show how the circular anchor reaches the deep failure mechanism at a lower embedment ratio than the strip anchor (*z/B*=9 for circular or axial symmetry, *z/B*=50 for strip or plane strain). Moreover, the maximum value for deep failure is 12% higher in axial symmetry than in plane strain in rough interface anchors and 8% higher in smooth interface anchors. This difference responds to the failure geometry in plane strain, with an infinite dimension in the anchor plate.

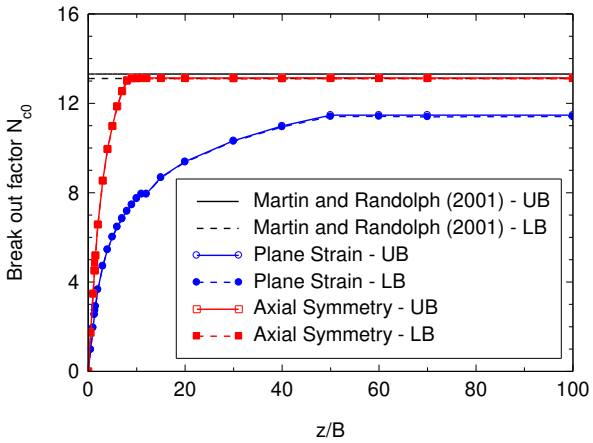

Figure 4. Break out factor in rough interface plate anchors (UB: upper bound, LB: lower bound).

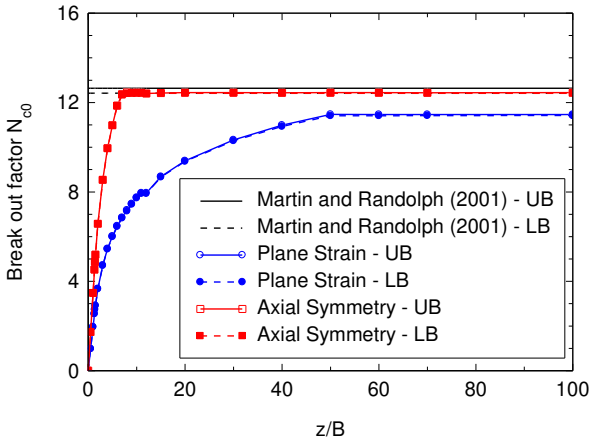

Figure 5. Break out factor in smooth interface plate anchors (UB: upper bound, LB: lower bound).

These figures also show the values of the N^*_{c0} factor presented by Martin and Randolph (2001) for rough and smooth interfaces. It can be observed that the lower bound values obtained from the calculations done in axial symmetry are practically equal to those offered by Martin and Randolph (2001). The results of in this study are more accurate since the difference between the upper and lower bound is lower. Seeing the results summarized in Table 1, the exact solution is between the upper bound value obtained in this study and the lower bound value obtained by Martin and Randolph (2001).

4.2 Three-dimensional analyses

Given the higher computational cost of three-dimensional calculations, less cases have been analysed. Figure 6 shows the results of the upper and lower bound analyses for rough interface square and circular anchors, contrasted with the N^*_{c0} values from Martin and Randolph (2001). Table 1 also shows the numerical value of the maximum break out factor for both shapes in three dimensions alongside the axial symmetric value and Martin and Randolph (2001).

Table 1. Maximum break out factor (N^*_{c0}) for both anchor shapes with rough interface and the values obtained by Martin and Randolph (2001).

	LB	**UB**	**Difference (%)**
Square 3D	11.98	12.71	5.7
Circular 3D	12.43	13.30	6.5
Martin and Randolph (2001)	13.11	13.31	1.5
Axial symmetry	13.1	13.14	0.5

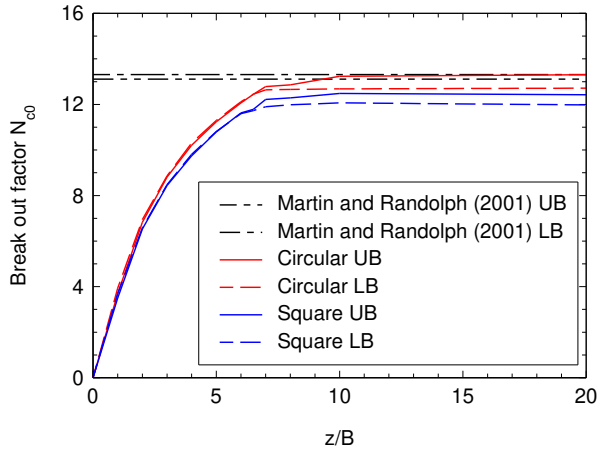

Figure 6. Break out factor for circular and square anchors in three dimensions. Comparison between results from OPTUMG3 and Martin and Randolph (2001) for rough interface anchors.

4.3 Shape influence

Figure 6 illustrates the differences in break out factor values for different shapes. For reduced embedment ratios, the vertical pull-out capacity in square and circular anchors is similar, being slightly higher for square anchors. However, for larger depths, where the deep failure mechanism has developed, the circular anchors show a better vertical pull-out capacity.

4.4 Failure mechanism

Figure 7 shows the failure mechanisms for two calculation cases in plane strain at different embedment depths, namely *z/B*=1.3 and 1.4. The upper part shows the finite

element mesh at the moment of failure. The lower part shows the shear dissipation, defined by Equation (7):

$$D_S = \int_V \sigma_S^T \, d\varepsilon_S^P \, dV \qquad (7)$$

where σ_S^T is the deviatoric stress, ε_S^P the deviatoric strain and V the volume. This is the parameter than code OPTUM uses to regulate the finite element mesh adaptivity (Krabbenhoft et al. 2015).

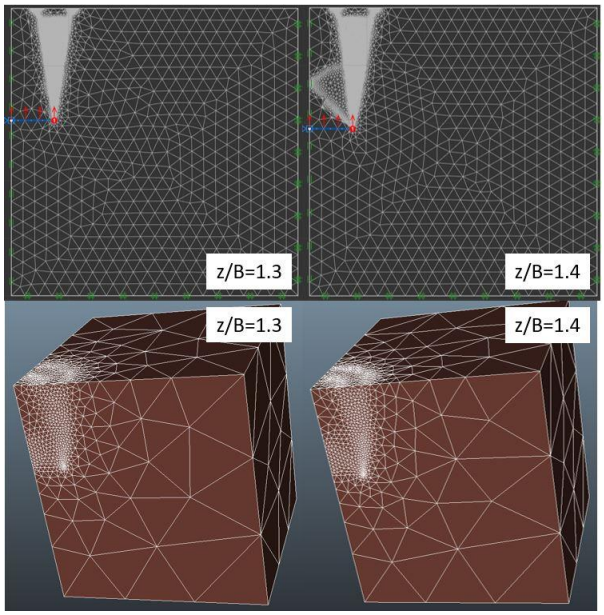

Figure 7. FE mesh at the moment of failure for 2D plane strain (upper) and 3D circular (lower) models. Rough interface, upper bound analysis.

The cases presented in Figure 7 are for two similar embedment depths and it can be appreciated how the failure mechanism varies with the shape (plane strain and circular). For plain strain conditions, at *z/B*=1.3 the failure lines are straight and correspond to a superficial failure mechanism However, at *z/B*=1.4 these lines start to curve, and a passive wedge is formed, at a 45° angle from the side of the anchor. It can be seen how the change from superficial to intermediate failure mechanism is not equal for circular anchors. For the same embedment depths, different results are obtained. This figure also illustrates the higher definition and precision that is obtained from the 2D model compared with the 3D model.

Table 2 presents break out factor values for superficial embedment depths obtained in this study compared with the expression proposed by Martin (2009) and the results of its finite element limit analyses done as well by Martin (2009). The analytical expression represents adequately the linear increase of break out factor. However, after a certain embedment depth (Figure 7) the failure mechanism is not superficial, and the analytical solution does not represent the real behaviour. The numerical analyses performed in this study concur with the results from Martin (2009) (Table 2).

Table 2. Superficial break out factor values from the solutions proposed by Martin (2009) (analytical and numerical) and from this study in plane strain conditions for rough anchors.

z/B	0.5	1	1.3	1.4	1.5	2
Slipline Eq.3	0.98	1.96	2.54	2.74	2.93	3.91
M (2009) UB	0.98	1.96	2.55	2.74	2.92	3.67
M (2009) LB	0.98	1.95	2.54	2.73	2.91	3.65
PS – UB	0.98	1.96	2.55	2.74	2.92	3.67
PS – LB	0.98	1.95	2.54	2.73	2.91	3.66

M (2009) = Martin (2009); PS = Plane Strain

For the following calculations, at increasing embedment depths, an intermediate failure mechanism is developed. It reaches the surface and expands laterally more than 3 times the length of the anchor side (*B*). Moreover, it can be seen how a localized plastic failure is generated at the side of the plate. Finally, the deep failure mechanism is fully developed. It is characterized for not reaching the surface, being localized around the tip of the plate and for corresponding to the maximum value of the break out factor (Figure 8). For embedment depths larger, the mechanism is the same and the results of the numerical analyses show it, as can be seen in Figure 4 to Figure 6.

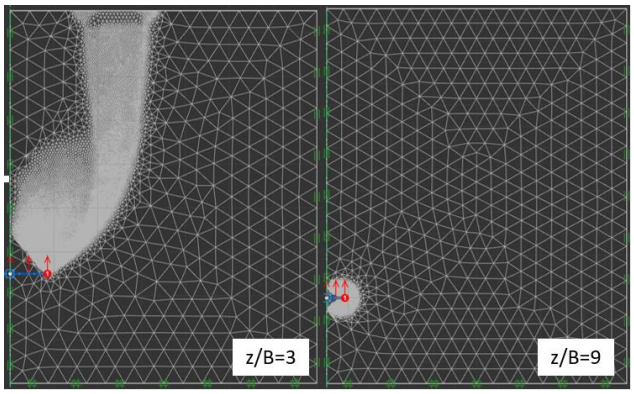

Figure 8. Mesh visualization of the intermediate mechanism (left) and deep failure mechanism (right). Upper bound, axial symmetry, rough interface.

4.5 Roughness influence

In this study, two extreme anchor surface roughness cases have been proposed. The expected result in a real-life case or in laboratory tests is an intermediate behaviour. This analysis was done in two dimensions. Table 3 shows the results of the analyses in axial symmetry (since it reaches the failure mechanism at lower embedment depths and more clearly) and the limiting values of the break out factor obtained by Martin and Randolph (2001) for rough and smooth anchors, also in axial symmetry.

Table 3. Summary of the results of the 2D analyses of roughness in circular anchors.

	N_{c0}
Rough LB (2D)	13.10
Rough UB (2D)	13.14
Martin and Randolph (2001) Rough LB	13.11
Martin and Randolph (2001) Rough UB	13.31
Smooth LB (2D)	12.42
Smooth UB (2D)	12.44
Martin and Randolph (2001) Smooth LB	12.42
Martin and Randolph (2001) Smooth UB	12.64

It can be observed how with the numerical analyses a higher precision was reached, given that the difference between the upper and lower bound solutions is lower than in other publications. The vertical pull-out force is higher in rough anchors than in smooth anchors. This is due to the rough anchor retaining more soil on its top side as it is driven upwards. In smooth anchors this soil would slide off more easily, reducing the load.

Finally, after analysing the results, it can be concluded that the exact solution will be closer to the lower bound solution than the upper bound.

5 CONCLUSIONS

The behaviour of plate anchors varies with the shape in a subtle manner. There are various analytical solutions that study their behaviour at different embedment depths. In order to compare them, a dimensionless factor is used, the break out factor N_{c0}. Several authors have given expressions that represent its variation with depth, anchor shape and, also, maximum values that correspond with a deep failure mechanism.

With the numerical analysis code OPTUM, in its both versions in 2D and 3D, a series of analyses have been done. Finite element limit analyses for plate anchors in two shapes were performed at different depths, obtaining upper and lower bound solutions. A good precision is reached, being better in two dimensional analyses than in three dimensions (due to the size of the model and the computational cost that it requires). The created model is validated by comparing the results with solutions proposed by other authors and can be applied for further research on the behaviour of different anchor shapes (square and circular), for a study regarding the behaviour at shallow or deep depths and, also, for an analysis on the influence of surface roughness.

The use of the numerical codes OPTUMG2 and OPTUMG3 offer two advantages: on the one hand, it allows performing upper and lower bound limit analyses; and, on the other hand, it offers a tool for adaptive mesh refinement that improves the performance of the numerical calculations. Therefore, it improves the precision of the model where the shear dissipation occurs.

6 ACKNOWLEDGEMENTS

The authors acknowledge financial support from the Spanish Ministry of Economic Affairs and Digital Transformation (MINECO) and the European Regional Development Fund (ERDF) through the project “Foundation of Offshore Platforms for Renewable Energies” (PEJ2018-003335-A) with financial resources from the Youth Employment Initiative (YEI) and the European Social Fund (ESF).

7 REFERENCES

Cañizal, F., Castro, J., Cañizal, J., Sagaseta, C. 2020. Pull-out capacity and failure mechanisms of strip anchors in clay, *Energies* **13**(3853).

Davis, E., 1968. Theories of plasticity and the failure of soil masses. *Soil mechanics: selected topics* (ed. I. K. Lee), 341-380.

Drucker, D., Greenberg, H., Prager, W. 1952. Extended limit design theorems for continuous media, *Quarterly J. Math* **9**, 381-389.

Krabbenhoft, K., Lyanmin, A., Krabbenhoft, J. 2015. Optum Computational Engineering (OptumG2). Optum, https://optumce.com , s.l.: s.n.

Lyamin, A. 1999. *Three-dimensional lower bound limit analysis using nonlinear programming,* Dept. of Civil, Surveying and Environmental Engineering, University of Newcastle, NSW, Australia.

Martin, C., 2009. Undrained collapse of a shallow plane-strain trapdoor, *Géotechnique* **59 (10)**, 855-863.

Martin, C., Randolph, M. 2001. Applications of the lower and upper bound theorems of plasticity to collapse of circular foundations. *Proc. 10th Int. Conf. on Computer Methods and Advances in Geomechanics,* **2**, 1417-1428.

Merifield, R., Lyanmin, A., Sloan, S., Yu, H. 2003. Three-dimensional lower bound solutions fro stability of plate anchors in clay. *Jornal of Geotechnical Engineering* **129(3)**, 243-253.

Merifield, R., Sloan, S., Yu, H. 2001. Stability of plate anchors in undrained clay. *Geotechnique* **51(2)**, 141-153.

Randolph, M., Gouvernec, S. 2011. *Offshore Geotechnical Engineering*. New York: Spon Press.

Rowe, R., Davis, E. 1982. The behaviour of anchor plates in clay. *Géotechnique* **32(1)**, 9-23.

Roy, A., Bhattacharya, P. 2020. Diameter effect on uplift capacity of horizontal circular anchor embedded in sand. *International Journal of Geotechnical Engineering* **14(7)**, 779-792.

Yu, L., Liu, J., Kong, X.-J., Hu, Y. 2011. Numerical study on plate anchor stability in clay. *Géotechnique* **61(3)**, 235-246.